

Quantitative Analysis of Intraventricular Dyssynchrony Using Wall Thickness by Multidetector Computed Tomography

Quynh A. Truong, MD,* Jagmeet P. Singh, MD, DPHIL,† Christopher P. Cannon, MD,‡
Ammar Sarwar, MD,* Khurram Nasir, MD, MPH,* Angelo Auricchio, MD, PhD,§
Francesco F. Faletra, MD,§ Antonio Sorgente, MD,§ Cristina Conca, MD,§
Tiziano Moccetti, MD,§ Mark Handschumacher, BS,† Thomas J. Brady, MD,*
Udo Hoffmann, MD, MPH*

Boston, Massachusetts; and Lugano, Switzerland

OBJECTIVES We sought to determine the feasibility of cardiac computed tomography (CT) to detect significant differences in the extent of left ventricular dyssynchrony in heart failure (HF) patients with wide QRS, HF patients with narrow QRS, and age-matched controls.

BACKGROUND The degree of mechanical dyssynchrony has been suggested as a predictor of response to cardiac resynchronization therapy. There have been no published reports of dyssynchrony assessment with the use of CT.

METHODS Thirty-eight subjects underwent electrocardiogram-gated contrast-enhanced 64-slice multidetector CT. The left ventricular endocardial and epicardial boundaries were delineated from short-axis images reconstructed at 10% phase increments of the cardiac cycle. Global and segmental CT dyssynchrony metrics that used changes in wall thickness, wall motion, and volume over time were assessed for reproducibility. We defined a global metric using changes in wall thickness as the dyssynchrony index (DI).

RESULTS The DI was the most reproducible metric (interobserver and intraobserver intraclass correlation coefficients ≥ 0.94 , $p < 0.0001$) and was used to determine differences between the 3 groups: HF-wide QRS group (ejection fraction [EF] $22 \pm 8\%$, QRS 163 ± 28 ms), HF-narrow QRS (EF $26 \pm 7\%$, QRS 96 ± 11 ms), and age-matched control subjects (EF $64 \pm 5\%$, QRS 87 ± 9 ms). Mean DI was significantly different between the 3 groups (HF-wide QRS: 152 ± 44 ms, HF-narrow QRS: 121 ± 58 ms, and control subjects: 65 ± 12 ms; $p < 0.0001$) and greater in the HF-wide QRS ($p < 0.0001$) and HF-narrow QRS ($p = 0.005$) groups compared with control subjects. We found that DI had a good correlation with 2-dimensional ($r = 0.65$, $p = 0.012$) and 3-dimensional ($r = 0.68$, $p = 0.008$) echocardiographic dyssynchrony.

CONCLUSIONS Quantitative assessment of global CT-derived DI, based on changes in wall thickness over time, is highly reproducible and renders significant differences between subjects most likely to have dyssynchrony and age-matched control subjects. (J Am Coll Cardiol Img 2008;1:772–81)

© 2008 by the American College of Cardiology Foundation

From the *Cardiac MR PET CT Program and the †Division of Cardiology, Massachusetts General Hospital, Harvard Medical School, Boston, Massachusetts; ‡Cardiovascular Division, Brigham and Women's Hospital, Harvard Medical School, Boston, Massachusetts; and §Cardiocentro Ticino, Lugano, Switzerland. Drs. Truong and Nasir received support from NIH grant T32HL076136. Dr. Auricchio is a consultant for GE Healthcare.

Manuscript received March 27, 2008; revised manuscript received June 11, 2008, accepted July 24, 2008.

Cardiac resynchronization therapy (CRT) has gained wide acceptance as adjunctive therapy with optimal medical treatment for the subgroup of patients with refractory heart failure (HF) (1,2). However, approximately 30% of patients who receive CRT had either no improvement or worsening of symptoms (3). The degree of intraventricular (or left ventricular [LV]) dyssynchrony has been suggested to be a major factor that affects CRT response (3,4).

This hypothesis has been supported by the results of small studies that suggest an association between the extent of LV dyssynchrony and clinical response to CRT (5-18). With the improved spatial and temporal resolution, cardiac computed tomography (CT) permits an accurate and reproducible 3-dimensional (3D) assessment of LV contractile function (19). These functional datasets also permit the analysis of wall thickness, wall motion, and volume over time and thus may be used to assess LV dyssynchrony. To date, there have been no published reports of LV dyssynchrony assessment in which the authors used either CT or wall thickness-based analysis.

Thus, the aims of this study were: 1) to evaluate the reproducibility of various novel CT-based measures of LV dyssynchrony, including global and segmental dyssynchrony metrics; and 2) to determine whether it is feasible to use a cardiac CT-based "dyssynchrony index," which uses changes in wall thickness, to detect significant differences in the extent of LV dyssynchrony between patients meeting CRT criteria (HF-wide QRS), age-matched control subjects, and a third group (HF-narrow QRS).

METHODS

Study population. For this case-control study, we selected 38 patients, based on echocardiography ejection fraction (EF) and electrocardiography (ECG) QRS duration, from the CT databases (between March 2005 and July 2007) of Massachusetts General Hospital-MGH, Boston, Massachusetts, and Cardiocentro Ticino-FCCT, Lugano, Switzerland. All patients must have had an echocardiogram, ECG, and multidetector CT performed. We queried our databases to find patients who met our criteria for HF-wide QRS criteria (EF $\leq 35\%$, QRS ≥ 120 ms), then we matched the HF-narrow QRS and control groups to age and gender. The control group had both normal LV function and QRS duration. Patients were classified

as the following groups: 1) HF-wide QRS: EF $\leq 35\%$, QRS ≥ 120 ms (echocardiography and ECG criteria for CRT); 2) HF-narrow QRS: EF $\leq 35\%$, QRS < 120 ms; or 3) age-matched control subjects: EF $> 55\%$, QRS < 120 ms. The study was approved by both institutional review boards.

Acquisition of CT and measurement. All subjects underwent standard ECG-gated contrast-enhanced 64-slice cardiac multidetector CT for routine CT coronary angiography per departmental protocol. The CT images were acquired during an inspiratory breath-hold with patients in the supine position. Intravenous beta-blockers for heart rate > 65 beats/min and sublingual nitroglycerin were used if not contraindicated. Image acquisition was performed with either Sensation 64 (Siemens Medical Solutions, Forchheim, Germany) or GE MSCT LightSpeed VCT (General Electric Healthcare, Milwaukee, Wisconsin) with the following parameters: 0.6- to 0.625-mm slice thickness, tube voltage 120 kVp, maximum tube current 850 mAs, gantry rotation time 330 to 350 ms. Pitch was dependent on patient's heart rate, and tube modulation was optional. Test bolus injection and total iodinate contrast were given at a rate of 5 ml/s, followed by saline infusion, with total contrast volume dependent on scan range.

After the scan, axial multiphase reformats (5% to 95%, 10% interval, total of 10 phases) were constructed with the Leonardo (Siemens Medical Solutions) or GE Advantage workstation (General Electric Healthcare, Paris, France). All patient information was de-identified, and the axial multiphase reformats dataset was recorded on a compact disc and sent to MGH Cardiovascular CT Core Lab for off-line postprocessing analyses.

All measurements were performed by 2 independent readers (Q.T. and A.S.). The axial CT images were reformatted into 8-mm thick short-axis images of the LV using QMassCT (Medis Medical Imaging Systems, Leiden, the Netherlands). The endocardial and epicardial boundaries of the LV were delineated manually in a semiautomated fashion (automated detection by the software algorithm with extensive manual correction for each phase and each slice of the left ventricle) and excluded the LV outflow tract, apical cap, and papillary muscles (Fig. 1). Observer 1 performed the reconstructions and measurements on all patients once. For interobserver and intraobserver reproducibility, Observer 2 performed the reconstructions and measurements in

ABBREVIATIONS AND ACRONYMS

2D	= two-dimensional
3D	= three-dimensional
CAD	= coronary artery disease
CRT	= cardiac resynchronization therapy
CT	= computed tomography
DI	= dyssynchrony index
ECG	= electrocardiography
EF	= ejection fraction
HF	= heart failure
ICC	= intraclass correlation coefficient
LV	= left ventricular

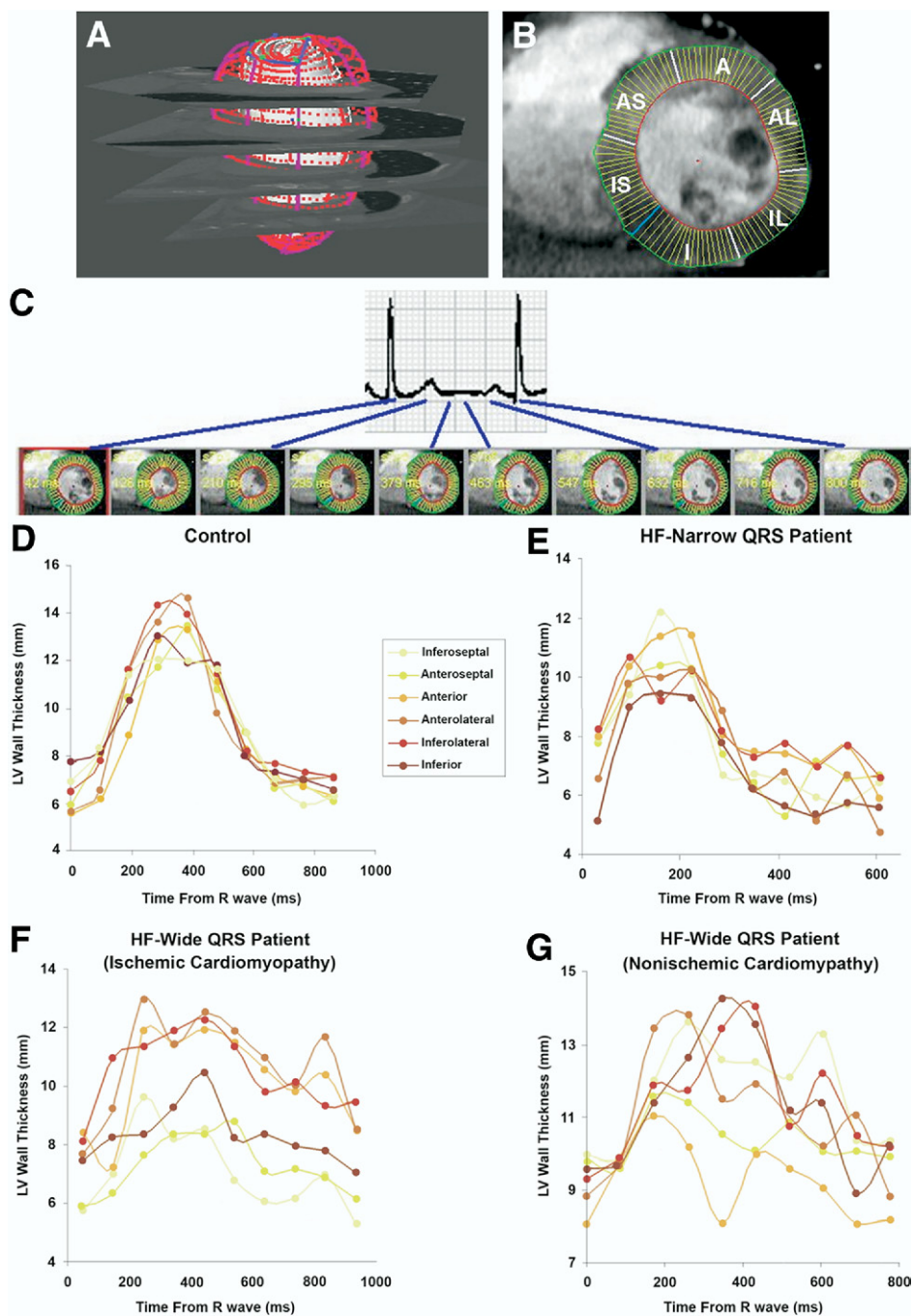


Figure 1. Method of Assessing Dyssynchrony With Wall Thickness Analysis by Cardiac CT

(A) Left ventricular (LV) model displaying short axis slices with endocardial (white) and epicardial (red dots) casts. (B) Endocardial (red) and epicardial (green) tracing of 1 short-axis image, segmented into 6 standardized segments. Left ventricular wall thickness is depicted as the radial distance between the endocardial and epicardial contours (yellow lines). (C) Serial short axis images depicted at 10% phase increments of the cardiac cycle at 1 slice level of the mid-ventricle. Representative graphs showed the time-to-maximal LV wall thickness at 1 ventricular slice in (D) a healthy "control" with EF 66%; (E) "HF-narrow QRS patient" with nonischemic cardiomyopathy and EF 31%; (F) "HF-wide QRS patient" with ischemic cardiomyopathy, EF 33%, and LBBB; and (G) "HF-wide QRS patient" with nonischemic cardiomyopathy, EF 19%, and LBBB. The graphs displayed the wall thickness of the 6 standardized segments of the LV myocardium over 1 cardiac cycle at a single ventricular slice level. The time-to-maximal wall thickness of the 6 segments is more variable in the HF-wide QRS patients than control and HF-narrow QRS, suggesting a greater degree of dyssynchrony. A = anterior; AL = anterolateral; AS = anterosseptal; CT = computed tomography; EF = ejection fraction; HF = heart failure; I = inferior; IL = inferolateral; IS = inferoseptal; LBBB = left bundle branch block.

20 randomly selected patients, and Observer 1 repeated this process in 20 patients 1 month later, respectively.

Derivation of CT-based metrics of LV dyssynchrony. The following global and/or segmental dyssynchrony metrics were defined by the following measurements: time-to-maximal wall thickness, time-to-maximal wall motion, and time-to-minimum volume.

TIME-TO-MAXIMAL WALL THICKNESS. Wall thickness was computed as the radial distance in millimeters between the endocardial and epicardial borders. The time from R-wave to maximal wall thickness was determined for each of the 6 standardized segments for all slices. For the global analyses, 2 metrics were derived: 1) the standard deviation (SD) of the time-to-maximal wall thickness of the 6 segments per slice averaged for all slices, which we defined as the dyssynchrony index (DI); and 2) the maximum difference in time-to-maximal wall thickness of all 3 pairs of opposing walls for all slices. For the segmental analyses, the maximum difference in time-to-maximal wall thickness of each of the opposing wall pairs was analyzed separately. On average, 540 data points (9 ± 3 slices, 6 segments, 10 phases) were analyzed per patient for each of the global wall thickness metrics; and 180 data points (9 ± 3 slices, 2 segments, 10 phases) were analyzed for the segmental ones.

TIME-TO-MAXIMAL WALL MOTION. Wall motion indicated the amount of movement of the wall and is computed by using the centerline algorithm as the radial distance from the centerline between the endocardial contours in the end-diastolic and end-systolic phases, with the end-diastolic phase as a reference. Modified from cardiac magnetic resonance imaging (15), we determined the time from R-wave to maximal wall motion for each of the 6 standardized segments for all slices. Similar to the wall thickness analyses but using endocardial boundaries only, the average of the SD and maximum difference in time-to-maximal wall motion of all segments and slices were calculated for global analyses, and the maximum difference in time between each of the 2 opposing walls was analyzed separately for segmental analyses. On average, 480 data points (9 ± 3 slices, 6 segments, 9 phases) were analyzed for global wall motion metrics, and 160 data points (9 ± 3 slices, 2 segments, 9 phases) were analyzed for segmental wall motion metrics.

TIME-TO-MINIMUM VOLUME. Volume was computed by using modified Simpson's method of disks with the LV endocardial area. Modified from 3D

echocardiography (14), we used data from endocardial contours. The time from R-wave to minimum systolic area was determined for all slices. The SD of these time-to-minimum volume is the derived global metric using volume. On average, 90 data points (9 ± 3 slices, 10 phases) were analyzed per patient for this metric.

Echocardiographic assessment. All patients underwent standard 2-dimensional (2D) echocardiography for dimensions, volumes, and EF that used commercially available hardware and software (Vivid 7, General Electric Vingmed Ultrasound, Horten, Norway). In 14 patients, 2D and 3D echocardiography dyssynchrony assessments were obtained. Speckle tracking 2D datasets were analyzed off-line using a software package (EchoPac 6.0.1, GE Vingmed Ultrasound). Real-time 3D echocardiography was performed with a 3V transducer and off-line analysis with 4D-LV software (Tom Tec Imaging Systems, Unterschleissheim, Germany).

LV diameters, volumes, and EF were measured by M-mode and biplane method of discs according to the guidelines of the American Society of Echocardiography (20). Speckle tracking 2D analysis, defined as the SD of the time to the first peak negative value of the longitudinal deformation, was performed from apical views (4-chamber, 2-chamber and long-axis) as previously described in details (9,21-23). The 3D echocardiography systolic dyssynchrony index was evaluated according to Kapetanakis et al. (14).

Statistical analysis. Continuous variables were expressed as mean \pm SD. Nominal variables were expressed as percentages. Differences in patient characteristics between the 3 groups were determined using analysis of variance for continuous and chi-square for categorical variables. Interobserver and intraobserver agreements of global and segmental LV dyssynchrony metrics were assessed with the intraclass correlation coefficient (ICC), Pearson's correlation coefficient, and Bland-Altman graphs. The paired *t* test was used to determine the significance for mean absolute and relative differences. The significance of differences in DI between the 3 groups was determined with analysis of variance. Two group comparisons were performed with unpaired *t* tests. Stratified analyses within HF-wide QRS group were performed using unpaired *t* tests. Correlation between DI and echocardiography dyssynchrony measures were assessed with Pearson's correlation coefficient. A 2-tailed *p* value <0.05 was considered significant. Statistical analysis was performed with STATA 10 (Stata Corp., College Station, Texas) and SPSS 16.0 (SPSS Inc., Chicago, Illinois).

Table 1. Patient Characteristics of the 3 Groups

	HF-Wide QRS EF ≤35%, QRS ≥120 ms (n = 16)	HF-Narrow QRS EF ≤35%, QRS <120 ms (n = 11)	Control EF >55%, QRS <120 ms (n = 11)	p Value
Patient characteristics				
Age, yrs	63 ± 15	57 ± 18	60 ± 11	NS
Gender, male (%)	11 (69)	9 (82)	9 (82)	NS
BMI, kg/m ²	26.3 ± 3.7	26.0 ± 5.7	25.4 ± 1.9	NS
Diabetes (%)	4 (25)	3 (27)	1 (9)	NS
Hypertension (%)	8 (50)	8 (73)	7 (64)	NS
CAD (%)	9 (56)	6 (55)	5 (45)	NS
NYHA functional class (%)				
I	0	4 (36)	11 (100)	<0.001
II	7 (44)	4 (36)	0	
III	9 (56)	3 (27)	0	
ECG parameters				
QRS duration (ms)	163 ± 28	96 ± 11	87 ± 9	<0.0001
LBBB (%)	7 (44)	0	0	0.003
Paced rhythm (%)	7 (44)	0	0	0.003
Heart rate during CT scan (beats/min)	69.2 ± 10.4	67.0 ± 13.8	67.7 ± 3.9	NS
Echocardiography parameters				
EF (%)	22 ± 8	26 ± 7	64 ± 5	<0.0001
LV dimensions, mm				
End-diastole (EDD)	63.1 ± 8.5	55.3 ± 8.2	49.4 ± 3.2	0.0001
End-systole (ESD)	56.8 ± 8.7	47.8 ± 9.4	27.5 ± 7.0	<0.0001
LV volumes, cm ³				
End-diastole (EDV)	274.1 ± 117.8	216.5 ± 73.5	85.8 ± 20.4	<0.0001
End-systole (ESV)	206.5 ± 88.5	163.6 ± 74.5	31.5 ± 11.4	<0.0001

BMI = body mass index; CAD = coronary artery disease; CT = computed tomography; EF = ejection fraction; HF = heart failure; NYHA = New York Heart Association; LBBB = left bundle branch block; LV = left ventricular; NS = nonsignificant.

RESULTS

The patient demographics, ECG findings, and echocardiography parameters are shown in Table 1. There are no significant differences with respect to age, gender, body mass index, and the presence of traditional cardiac risk factors (diabetes, hypertension, or coronary artery disease [CAD]) between the 3 groups. As expected, ECG and echocardiography parameters are significantly different between the 3 groups, except for the heart rate during the CT scan acquisition. The average heart rate during the CT scan was 68.1 ± 10.0 beats/min. Additionally, the HF-wide QRS group has worse New York Heart Association functional class status compared with HF-narrow QRS and controls.

Reproducibility of CT-based metrics of LV dyssynchrony. Table 2 depicts the interobserver and intraobserver variability of CT dyssynchrony metrics derived from assessment of wall thickness, wall motion, and volume in a global and/or segmental basis. Overall, global dyssynchrony measurements (ICC range 0.71 to 0.95) were more reproducible

than segmental metrics (ICC range 0.06 to 0.91). Of the global metrics, the measurements of changes in wall thickness (ICC range 0.90 to 0.95) were more reproducible than measurements utilizing changes in wall motion (ICC range 0.80 to 0.92) or volume (ICC range 0.71 to 0.78).

Computed tomography dyssynchrony index. The global LV dyssynchrony metric using changes in LV wall thickness over time (average of the SD of 6 segments per slice, using all slices) had the best reproducibility with excellent interobserver and intraobserver reproducibility (ICC of 0.94 and 0.95, respectively, both $p < 0.0001$) and was defined as the CT dyssynchrony index (DI). The correlation coefficient ($r = 0.93$, $p < 0.0001$) between individual DI measurements by Observer 1 and 2 was excellent (Fig. 2A). No systematic bias was observed between the 2 observers' measurements by Bland-Altman analysis (Fig. 2B).

The mean DI was significantly different between the 3 groups ($p < 0.0001$) (Fig. 3). For the HF-wide QRS group, the mean DI was 152 ± 44 ms, range 62 to 226 ms. For the HF-narrow QRS group, the mean DI was 121 ± 58 ms, range 58 to

Table 2. Interobserver and Intraobserver Reproducibility of CT-Based Dyssynchrony Metrics

Dyssynchrony Metrics	Interobserver Variability			Intraobserver Variability		
	Mean Actual Difference (ms)	Percentage Difference (%)	ICC	Mean Actual Difference (ms)	Percentage Difference (%)	ICC
Time-to-maximal wall thickness						
Global						
Average of SD of 6 segments of all slices (DI)	5.8 ± 27.0	0.06 ± 0.26	0.94	1.8 ± 24.3	0.02 ± 0.23	0.95
Maximum difference of all 3 pairs of opposing walls	40.4 ± 122.7	0.10 ± 0.32	0.90	30.4 ± 113.1	0.13 ± 0.50	0.92
Segmental						
Maximum difference of 2 opposing walls						
Anterior-inferior	47.4 ± 170.8	0.15 ± 0.55	0.76	1.9 ± 125.2	0.01 ± 0.40	0.87
Inferoseptal-anterolateral	36.2 ± 154.4	0.11 ± 0.47	0.78	54.1 ± 158.6	0.16 ± 0.48	0.75
Anteroseptal-inferolateral	23.8 ± 138.1	0.08 ± 0.45	0.80	8.4 ± 106.7	0.03 ± 0.34	0.91
Time-to-maximal wall motion						
Global						
Average of SD of 6 segments of all slices	0.6 ± 28.9	0.01 ± 0.36	0.83	7.0 ± 18.4	0.09 ± 0.23	0.92
Maximum difference of all 3 pairs of opposing walls	29.2 ± 133.0	0.09 ± 0.42	0.86	20.2 ± 133.8	0.07 ± 0.47	0.80
Segmental						
Maximum difference of 2 opposing walls						
Anterior-inferior	29.7 ± 215.0	0.13 ± 0.96	0.16 [‡]	4.5 ± 176.3	0.01 ± 0.45	0.06 [§]
Inferoseptal-anterolateral	19.7 ± 180.9	0.08 ± 0.75	0.68	25.3 ± 163.9	0.13 ± 0.83	0.66
Anteroseptal-inferolateral	8.5 ± 140.1	0.04 ± 0.60	0.74	18.0 ± 94.5	0.08 ± 0.43	0.84
Time-to-minimum volume						
Global						
SD of all slices	16.2 ± 25.6	0.26 ± 0.40*	0.78	12.3 ± 23.1	0.19 ± 0.36 [†]	0.71

Dyssynchrony metrics were defined using wall thickness, wall motion, and volume in a global and/or segmental basis. All global and segmental metrics included data from all slices, including the maximal difference measurements. All p values for the mean actual difference and percentage difference calculations were nonsignificant, except for *p = 0.01 and †p = 0.03. Interobserver and intraobserver reproducibility of each measure were reported as ICC with all p < 0.01, except for ‡p = 0.36 and §p = 0.45. The time-to-maximal wall thickness global metric using the average of the SD of 6 segments of all slices was defined as DI.
 DI = dyssynchrony index; ICC = intraclass correlation coefficient; other abbreviations as in Table 1.

203 ms. For the age-matched controls, the mean DI was 65 ± 12 ms, range 43 to 78 ms. The mean DI was significantly greater in the HF-wide QRS (p < 0.0001) and HF-narrow QRS (p = 0.005) groups when compared with control subjects, but there was no statistical difference between the 2 HF groups (p = 0.131). In secondary analyses there was no significant correlation between DI and EF (r = -0.27, p = 0.167) and only modest correlation between DI and QRS duration (r = 0.51, p = 0.007).

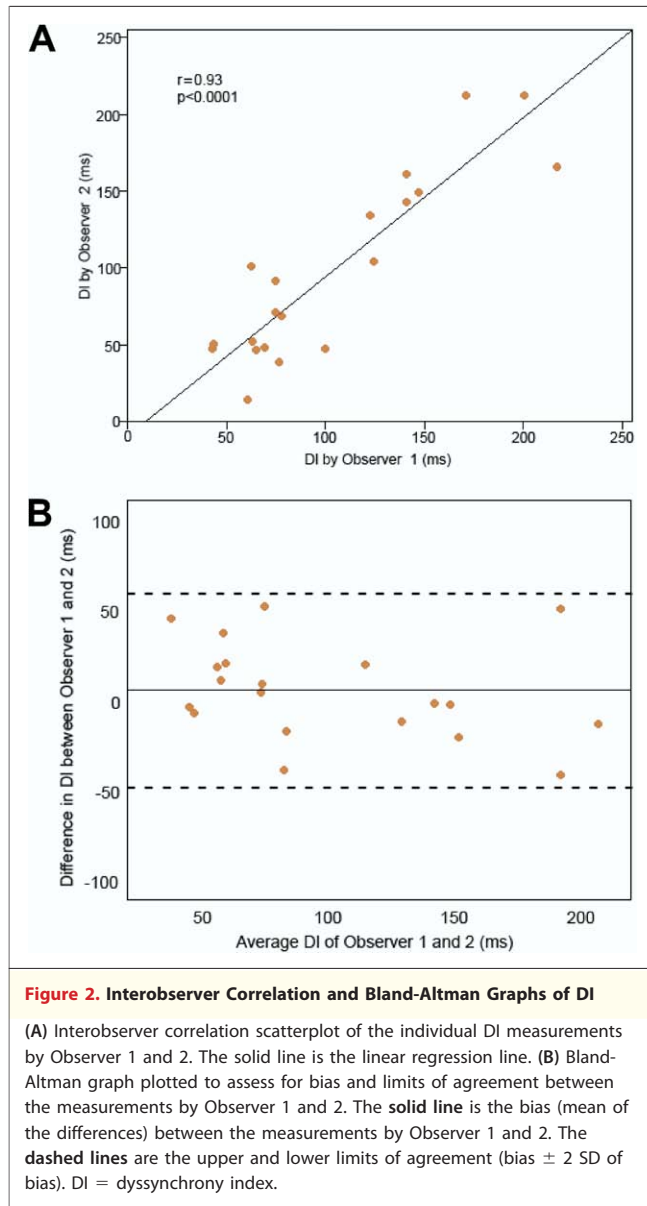
Among patients with wide QRS (Table 3), mean DI was significantly greater in those whose QRS duration was above the median of 161 ms (p = 0.04) and those with paced rhythm (p = 0.001) but did not differ when stratified by median EF of 19.5%, the presence of CAD, left bundle branch block, or New York Heart Association functional class. Within this group of patients with wide QRS, there also was no difference in mean DI between patients with end-diastolic and end-systolic diameters and end-diastolic and end-systolic volume

above the median compared to those below the median (data not shown).

Correlation of DI with echocardiography dyssynchrony measures. Of the 14 patients with CT, 2D echocardiography, and 3D echocardiography dyssynchrony assessments, the mean DI was 87 ± 48 ms, range 43 to 217 ms; mean 2D echocardiography speckle tracking strain was 51 ± 47 ms, range 18 to 166 ms; and mean 3D echocardiography dyssynchrony was 5.3 ± 5.2 ms, range 1.2 to 20.0 ms. The correlation between DI and 2D echocardiography dyssynchrony assessment when speckle tracking longitudinal strain was used was good (r = 0.65, p = 0.012). Similarly, there was good correlation between DI and 3D echocardiography dyssynchrony (r = 0.68, p = 0.008).

DISCUSSION

This is the first study to use 64-slice multidetector CT to quantify the degree of LV dyssynchrony. We provide an initial description of novel quantitative



CT analyses using changes in wall thickness, wall motion, and volume over time for the assessment of dyssynchrony. Our data demonstrate that global metrics are more reproducible than segmental ones and that wall thickness analysis is more reproducible than wall motion and volume methods. As a proof of principle, we further demonstrate that the DI, for which both endocardial and epicardial boundaries are used for wall thickness analysis, is significantly greater in subjects with heart failure and wide QRS compared with age-matched controls.

Reproducibility of CT dyssynchrony metrics. We provide a systematic assessment of the intraobserver and interobserver reproducibility of global- and

segmental-based measures of LV dyssynchrony. Our data demonstrate that global metrics of LV dyssynchrony are more reproducible than segmental-based metrics. Computed tomography dyssynchrony metrics based on wall thickness measurements were more reproducible compared with metrics based on wall motion and volume. The most reproducible CT dyssynchrony metric was the DI (ICC >0.94 , $p < 0.0001$ for both intraobserver and interobserver reproducibility), which is based on the measurement of changes in wall thickness over time. In contrast to published data in which the authors used cardiac magnetic resonance imaging and 3D echocardiography, which incorporated only the endocardial borders for dyssynchrony assessment (14,15), this DI is novel because it is the first dyssynchrony metric based on wall thickness, a measure that uses both endocardial and epicardial boundaries. Of note, this metric that uses wall thickness could be performed with cardiac magnetic resonance imaging, which also has excellent temporal resolution. Wall thickness analysis may allow for a more precise assessment of differences in wall mechanics and myocardial contractile force, allowing for comprehensive assessment of dyssynchrony.

Differences in CT dyssynchrony index between groups.

Our study demonstrates that it is feasible to detect significant differences in LV dyssynchrony between patients in the HF-wide QRS group, who fulfilled ECG and echocardiography criteria for CRT, and age- and gender-matched controls. The DI was significantly greater in the HF-wide QRS group (152 ± 44 ms) compared with control subjects (65 ± 12 ms, $p < 0.0001$). Moreover, there was a clear discrimination between these groups because all but 1 patient in the wide QRS group had a higher DI, reflecting a greater extent of LV dyssynchrony, when compared with control patients. This measure had good correlation with validated 2D (9, 21–23) and 3D echocardiography (14) dyssynchrony measures ($r = 0.65$ and $r = 0.68$, respectively), although there currently is no gold standard for dyssynchrony assessment (24).

We believe this CT-based LV DI may characterize patients, CRT eligibility beyond currently used measures of EF and QRS duration. Our data from secondary analyses among those with EF $\leq 35\%$ suggest that DI does not correlate with the degree of LV dysfunction ($r = -0.27$, $p = 0.167$) and only moderately correlates with QRS duration ($r = 0.51$, $p = 0.007$). Additionally, in our subgroup analysis of HF-wide QRS patients, there was no difference in DI between patients with ischemic and nonischemic cardiomyopathy; thus, our mea-

sure is not likely to be influenced by whether there are regional wall motion abnormalities as opposed to global hypokinesis. We also found that those patients who were paced during the CT scan had greater DI than those who were not ($p = 0.001$), which gives us further support that DI is a measure of dyssynchrony because right ventricular pacing is known to be associated with dyssynchrony (25,26). Moreover, although it may appear that DI as a standard deviation measure of wall thickness may represent measurement “noise” because impaired wall thickness may appear to be more difficult to measure in HF patients with systolic dysfunction than in control patients with normal myocardial thickening, this is not likely to be the case. In the HF-narrow QRS group, 4 of 11 patients had low DI values in the same range as the normal control group with $DI < 78$ ms, so our measure of DI cannot simply be attributed to measurement “noise” due to impaired LV thickening. As depicted in Figure 1, the HF patient with narrow QRS (Fig. 1E) had an EF of 31%, which is comparable with the HF patient with left bundle branch block (Fig. 1F) whose EF was 33%. Thus, we do not believe our metric is a measurement of “noise” because of low EF; instead, we believe it represents a difference in dyssynchrony.

In HF patients with narrow QRS duration, the role of dyssynchrony and CRT remains uncertain (27). In our study, the mean DI in the HF-narrow QRS group (121 ± 58 ms) is intermediate between the HF-wide QRS (152 ± 44 ms) and the control group (65 ± 12 ms, $p < 0.0001$), suggesting that some patients in this population may be identified as having a large degree of dyssynchrony using this metric (Fig. 3). However, CRT usage in this population remains controversial (27) and this metric will need to be validated in future studies in HF patients with wide QRS duration first.

Issue of temporal resolution. The temporal resolution of the 64-slice CT technology used in this study is relatively limited at 165 to 175 ms. For this temporal resolution 10% RR interval reconstructions (10 phases) for a mean heart rate of 68 beats/min during scanning is adequate. Although some authors propose to reconstruct at 5% increments of the RR interval (20 phases), the presumed increase in temporal resolution would be artificial. Although we are not advocating the use of 64-slice CT for dyssynchrony, we designed this study as a “proof of principle” to see whether we could detect a difference in DI between 2 extremes: HF-wide QRS and controls. Yet despite the poor temporal resolution,

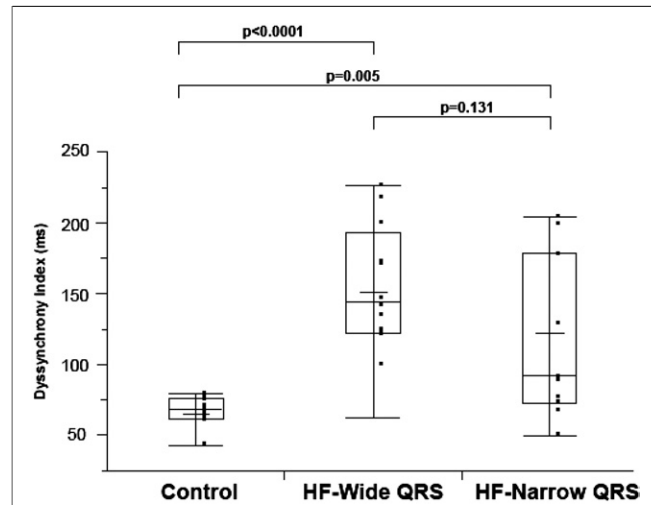


Figure 3. Box and Whisker Plot of DI Using Changes in LV Wall Thickness of the 3 Groups

Mean DI was significantly different between the 3 groups and was greatest in the HF-wide QRS group, followed by the HF-narrow QRS, and then the control group (152 ± 44 ms vs. 121 ± 58 ms vs. 65 ± 12 ms, respectively; $p < 0.0001$). HF = heart failure; LV = left ventricular; other abbreviations, as in Figure 2.

we were still able to discern a significant difference ($p < 0.0001$) between patients most likely to have dyssynchrony (HF-wide QRS) and matched controls. Thus, if we are able to discern a difference when we use the 64-slice CT scanner, then we should be able to discern a difference when we use newer CT scanner technology (i.e., dual-source CT), where the temporal resolution has dramatically improved to 83 ms with single segment reconstruction and reported to be up to 42 ms with a

Table 3. Subgroup Analyses of HF-Wide QRS Group

HF-Wide QRS Subgroups	n	Mean DI \pm SD (ms)	p Value
QRS >161 ms (median)	8	174 \pm 38	0.04
QRS <161 ms (median)	8	130 \pm 40	
Echocardiography			
EF <19.5 (median)	8	151 \pm 24	0.91
EF >19.5 (median)	8	153 \pm 60	
CAD			
No CAD	7	154 \pm 42	0.84
LBBB	7	133 \pm 47	0.12
No LBBB	9	167 \pm 37	
Paced rhythm	7	187 \pm 35	0.001
Not paced	9	125 \pm 28	
NYHA functional class			
II	7	142 \pm 50	0.42
III	9	160 \pm 40	

ECG = electrocardiography; SD = standard deviation; other abbreviations as in Tables 1 and 2.

mean temporal resolution of 60 ms when multisegment reconstruction algorithms are used (28). This temporal resolution is comparable to that of 3D echocardiography and cardiac magnetic resonance imaging and would be in the appropriate range for dyssynchrony assessment. With the better temporal resolution scanners, modifying our method by using 5% RR interval reconstructions (20 phases) instead of 10% would be adequate. Further research with improved CT temporal resolution scanners is needed to determine the utility of cardiac CT to identify subjects who may or may not benefit from CRT.

Potential role of CT and clinical implications. Advantages of CT over other noninvasive imaging modalities are less operator dependence, rapid imaging time, and most importantly simultaneous visualization of the coronary venous anatomy. Coronary venous anatomy imaging before device implantation is a unique feature to CT and may have the potential to integrate anatomic with functional data to guide optimal lead placement by targeting regions of most delayed activation and avoiding regions of myocardial scar.

A disadvantage of CT is the exposure to radiation and the consequent potentially increased risk of cancer. Although the issue of radiation and the risk of cancer from CT performed in low-risk normal patients for the evaluation of potential CAD is of recent concern (29), in our high-risk group of refractory HF patients with 50% 5-year mortality (30), judicious use of CT may have a favorable benefit-risk profile when being used to help guide appropriate use of CRT, a life-saving treatment. With the increasing use of gated cardiac CT preprocedurally to image the coronary sinus and cardiac veins to facilitate LV lead placement (31,32), functional data for dyssynchrony assessment is readily available for analysis to the physician at no additional cost of radiation to the patient and without a need for an extra test. As advanced CT technology continues to improve temporal resolution, minimize radiation, and expedite post-processing analyses, further research with CT is warranted in this patient population to optimize response to CRT.

Study limitations. The major limitation of the study is the small sample size. Thus, our findings should be interpreted as a “proof of principle,” which demonstrates the feasibility of this new method using CT and wall thickness analysis for assessing dyssynchrony. Because of a lack of a gold standard, although we believe that greater DI represents a greater extent of mechanical dyssynchrony, we cannot be certain of the causality. Additionally, our study did not address whether DI correlates with CRT response, and further prospective studies with higher temporal resolution CT scanners are needed to validate this metric. Furthermore, our subgroup analysis may be underpowered, and larger studies will need to ensue to further identify predictors of DI.

CONCLUSIONS

Cardiac CT permits the derivation of global- and segmental-based measures of LV dyssynchrony. We describe here a novel, reproducible quantitative CT-based method for dyssynchrony assessment using changes in wall thickness (i.e., DI) that allow for the detection of differences between subjects who most likely have dyssynchrony and age-matched control subjects. These results justify further research, specifically, prospective studies that use advanced CT technology with improved temporal resolution, to determine whether DI may predict response to CRT. Additionally, the ability to define the coronary venous anatomy beforehand is a unique feature of CT over other noninvasive modalities and provides a dual purpose—coronary veins and dyssynchrony assessment—for its potential use as a single imaging modality for CRT.

Acknowledgment

The authors thank Alexandra Hochmuth from Medis for technical support.

Reprint requests and correspondence: Dr. Quynh A. Truong, Cardiac MR PET CT Program, Massachusetts General Hospital, 165 Cambridge Street, Suite 400, Boston, Massachusetts 02114. *Email:* qtruong@partners.org.

REFERENCES

- Gregoratos G, Abrams J, Epstein AE, et al. ACC/AHA/NASPE 2002 guideline update for implantation of cardiac pacemakers and antiarrhythmia devices—summary article: a report of the American College of Cardiology/American Heart Association Task Force on Practice Guidelines (ACC/AHA/NASPE Committee to Update the 1998 Pacemaker Guidelines). *J Am Coll Cardiol* 2002;40:1703-19.
- Vardas PE, Auricchio A, Blanc JJ, et al. Guidelines for cardiac pacing and cardiac resynchronization therapy: the task force for cardiac pacing and cardiac resynchronization therapy of the European Society of Cardiology. Developed in collaboration with the European Heart Rhythm Association. *Eur Heart J* 2007;28:2256-95.
- Bax JJ, Abraham T, Barold SS, et al. Cardiac resynchronization therapy: part 1—issues before device implantation. *J Am Coll Cardiol* 2005;46:2153-67.

4. Bax JJ, Abraham T, Barold SS, et al. Cardiac resynchronization therapy: part 2—issues during and after device implantation and unresolved questions. *J Am Coll Cardiol* 2005;46:2168–82.
5. Notabartolo D, Merlino JD, Smith AL, et al. Usefulness of the peak velocity difference by tissue Doppler imaging technique as an effective predictor of response to cardiac resynchronization therapy. *Am J Cardiol* 2004;94:817–20.
6. Pitzalis MV, Iacoviello M, Romito R, et al. Cardiac resynchronization therapy tailored by echocardiographic evaluation of ventricular asynchrony. *J Am Coll Cardiol* 2002;40:1615–22.
7. Ansalone G, Giannantoni P, Ricci R, et al. Doppler myocardial imaging in patients with heart failure receiving biventricular pacing treatment. *Am Heart J* 2001;142:881–96.
8. Bax JJ, Ansalone G, Breithardt OA, et al. Echocardiographic evaluation of cardiac resynchronization therapy: ready for routine clinical use? A critical appraisal. *J Am Coll Cardiol* 2004;44:1–9.
9. Suffoletto MS, Dohi K, Cannesson M, Saba S, Gorcsan J, III. Novel speckle-tracking radial strain from routine black-and-white echocardiographic images to quantify dyssynchrony and predict response to cardiac resynchronization therapy. *Circulation* 2006;113:960–8.
10. Yu CM, Zhang Q, Fung JW, et al. A novel tool to assess systolic asynchrony and identify responders of cardiac resynchronization therapy by tissue synchronization imaging. *J Am Coll Cardiol* 2005;45:677–84.
11. Marcus GM, Rose E, Vilorio EM, et al. Septal to posterior wall motion delay fails to predict reverse remodeling or clinical improvement in patients undergoing cardiac resynchronization therapy. *J Am Coll Cardiol* 2005;46:2208–14.
12. Diaz-Infante E, Sitges M, Vidal B, et al. Usefulness of ventricular dyssynchrony measured using M-mode echocardiography to predict response to resynchronization therapy. *Am J Cardiol* 2007;100:84–9.
13. Yu CM, Fung JW, Zhang Q, et al. Tissue Doppler imaging is superior to strain rate imaging and postsystolic shortening on the prediction of reverse remodeling in both ischemic and nonischemic heart failure after cardiac resynchronization therapy. *Circulation* 2004;110:66–73.
14. Kapetanakis S, Kearney MT, Siva A, Gall N, Cooklin M, Monaghan MJ. Real-time three-dimensional echocardiography: a novel technique to quantify global left ventricular mechanical dyssynchrony. *Circulation* 2005;112:992–1000.
15. Chalil S, Stegemann B, Muhyaldeen S, et al. Intraventricular dyssynchrony predicts mortality and morbidity after cardiac resynchronization therapy: a study using cardiovascular magnetic resonance tissue synchronization imaging. *J Am Coll Cardiol* 2007;50:243–52.
16. Lardo AC, Abraham TP, Kass DA. Magnetic resonance imaging assessment of ventricular dyssynchrony: current and emerging concepts. *J Am Coll Cardiol* 2005;46:2223–8.
17. Teclao SR, Zwaneburg JJ, Kuijter JP, et al. Quantitative comparison of 2D and 3D circumferential strain using MRI tagging in normal and LBBB hearts. *Magn Reson Med* 2007;57:485–93.
18. Westenberg JJ, Lamb HJ, van der Geest RJ, et al. Assessment of left ventricular dyssynchrony in patients with conduction delay and idiopathic dilated cardiomyopathy: head-to-head comparison between tissue Doppler imaging and velocity-encoded magnetic resonance imaging. *J Am Coll Cardiol* 2006;47:2042–8.
19. Belge B, Coche E, Pasquet A, Vanoverschelde JL, Gerber BL. Accurate estimation of global and regional cardiac function by retrospectively gated multidetector row computed tomography: comparison with cine magnetic resonance imaging. *Eur Radiol* 2006;16:1424–33.
20. Schiller NB, Shah PM, Crawford M, et al. Recommendations for quantitation of the left ventricle by two-dimensional echocardiography. American Society of Echocardiography Committee on Standards, Subcommittee on Quantitation of Two-Dimensional Echocardiograms. *J Am Soc Echocardiogr* 1989;2:358–67.
21. Perk G, Tunick PA, Kronzon I. Non-Doppler two-dimensional strain imaging by echocardiography—from technical considerations to clinical applications. *J Am Soc Echocardiogr* 2007;20:234–43.
22. Reisner SA, Lysyansky P, Agmon Y, Mutlak D, Lessick J, Friedman Z. Global longitudinal strain: a novel index of left ventricular systolic function. *J Am Soc Echocardiogr* 2004;17:630–3.
23. Leitman M, Lysyansky P, Sidenko S, et al. Two-dimensional strain—a novel software for real-time quantitative echocardiographic assessment of myocardial function. *J Am Soc Echocardiogr* 2004;17:1021–9.
24. Chung ES, Leon AR, Tavazzi L, et al. Results of the Predictors of Response to CRT (PROSPECT) Trial. *Circulation* 2008;117:2608–16.
25. Vassallo JA, Cassidy DM, Miller JM, Buxton AE, Marchlinski FE, Josephson ME. Left ventricular endocardial activation during right ventricular pacing: effect of underlying heart disease. *J Am Coll Cardiol* 1986;7:1228–33.
26. Eldadah ZA, Rosen B, Hay I, et al. The benefit of upgrading chronically right ventricle-paced heart failure patients to resynchronization therapy demonstrated by strain rate imaging. *Heart Rhythm* 2006;3:435–42.
27. Beshai JF, Grimm RA, Nagueh SF, et al. Cardiac-resynchronization therapy in heart failure with narrow QRS complexes. *N Engl J Med* 2007;357:2461–71.
28. Flohr TG, McCollough CH, Bruder H, et al. First performance evaluation of a dual-source CT (DSC) system. *Eur Radiol* 2006;16:256–68.
29. Einstein AJ, Henzlova MJ, Rajagopalan S. Estimating risk of cancer associated with radiation exposure from 64-slice computed tomography coronary angiography. *JAMA* 2007;298:317–23.
30. Rosamond W, Flegal K, Friday G, et al. Heart disease and stroke statistics—2007 update: a report from the American Heart Association Statistics Committee and Stroke Statistics Subcommittee. *Circulation* 2007;115:e69–e171.
31. Auricchio A, Sorgente A, Singh JP, et al. Role of multislice computed tomography for preprocedural evaluation before revision of a chronically implanted transvenous left ventricular lead. *Am J Cardiol* 2007;100:1566–70.
32. Hemminger EJ, Girsky MJ, Budoff MJ. Applications of computed tomography in clinical cardiac electrophysiology. *J Cardiovasc Comput Tomography* 2007;1:131–42.

Key Words: imaging ■
tomography ■ heart failure ■
pacing ■ dyssynchrony.